Indian Journal of Engineering & Materials Sciences
Vol. 20, December 2013, pp. 504-514

Correlation of absorbed impact with calculated strain energy using an instrumented Charpy impact test

M B Ali[a,b]*, S Abdullah[a] , M Z Nuawi[a] & A K Ariffin[a]

[a]Department of Mechanical and Materials Engineering, Faculty of Engineering and Built Environment, Universiti Kebangsaan Malaysia 43600 Bangi, Selangor, Malaysia
[b]Department of Structure and Materials, Faculty of Mechanical Engineering, Universiti Teknikal Malaysia Melaka, Hang Tuah Jaya, 76100 Durian Tunggal, Melaka, Malaysia

Received 20 April 2012; accepted 23 July 2013

This paper presents the correlation of impact energy obtained from the laboratory test as well as the calculated energy using the power spectrum density (PSD) method. Based on a previous study, the total absorbed energy obtained using the dial/encoder system may be significantly different, depending on the strength and the ductility of test specimen. For this reason, we determined the energy of the experimental system coming from the dial/encoder Charpy impact test using the signal processing approach. Strain gauges are connected between the Charpy impact striker and the high frequency data acquisition system in order to capture the dynamic impact strain response. A specimen of an aluminium alloy of 6061-T6 is used in the experiment, which is designed according to the ASTM E23. For the analysis an obtained signal is converted from the time domain to the frequency domain by means of PSD method and the area under its plot is used to calculate strain energy. The comparison between energy absorbed during the experiment and the strain energy is performed at different velocities and thicknesses. The total energy absorbed using the dial/encoder system can be linked by a polynomial equation with R^2 of 99.8%. Thus, the effect of the strain signal pattern and impact duration with different velocities and thicknesses are correlated with energy from PSD. This suggests that velocity and thickness are important parameters to be considered in testing the material and finally this correlation can be used as an alternative.

Keywords: Charpy impact, Dial/encoder system, Energy, PSD, Signal, Strain

The testing of Charpy impact has been studied and applied for many years and has remained as one of the methods considered in examining the fracture toughness issue due to its low cost and reliability[1]. The amount of energy absorbed in a material can be measured by the Charpy v-notch test which is a standardised high strain rate test. The absorbed energy obtained using dial/encoder system is considered as a measurement of the material's toughness and react as a tool for the ductile-brittle transition with depend on the temperature during testing. The use of instrumented Charpy impact apparatus with the load-time recording system aims to determine the fracture energy and the general yielding of material, the maximum load applied on to the specimens, and finally the moment level of brittle fracture occurrence[2-4]. A general Charpy test instrument features the dial indicator and an optical encoder for the purpose of measuring the absorbed energy occurred during the impact. The total absorbed energies obtained using these technologies are generally in good agreement; however, significant differences in terms of amount can sometimes be recorded[5]. The total absorbed energy has been found higher or less than by using dial indicator or optical encoder, depending on the strength of material, ductility of test specimen and other factors[6]. According to Xu *et al.*[7], more than 80% of the absorbed energy is not accurate and calculated as an estimate.

Meanwhile, the dynamic responses from standard Charpy impact instrument have been experimentally studied by attached strain gauges and an accelerometer to the impact striker; the results in this work have also been validated with finite element analysis[8]. In that work, the first natural frequencies in the acceleration signal of the Charpy sample have high modal magnitudes, although they differed with strain gauges. Toshiro *et al.*[9] studied the strain gauge position and an effect of the striker shape on instrumented Charpy impact test, who found that the effect of the hammer vibration appeared to be

*Corresponding author (E-mail: abgbas@yahoo.com)

stronger around the end of the slit. Sahraoui and Laitailate[10] explained different materials with contact stiffness, such as the striker and the specimen. In addition, using the specific method to evaluate the load oscillation frequency, they found the interaction between the specimen and the striker reacts as a dominant in the effect of vibration and impact. Furthermore, Kondryakov *et al.*[11] studied a multichannel system of high-speed strains and loads recording process during the fracture toughness testing, with the strain gauges attached to the striker and to the specimen support. Their approach allowed the recording of information regarding specimen deformation occurring during the test. Francois and Pineau[5] studied an observation on differences between the energy measured by U-hammer on instrumented striker and dial/encorder energy. They obtain the energy of an instrumented striker by calculating the vibration energy (accelerometer data) using Fourier analysis is influenced or related to the absorbed energy. These results are potentially important, because the fracture energy for low energy of specimens is related with vibration energy.

The mechanical and electrical filtering effects have been evaluated for signals captured from strain gauge attached at a striker as performed by Aggag and Takahashi[12]. They chose two levels of thickness, i.e., 0.5 and 1.0 mm, in indicating the reduction of the inertial oscillation; they also improved the values of impact energy. The experiment was run at two different velocities, namely, 2.8 and 4.0 m/s. The response of the Michelson interferometric fibre-optic sensors to impact loading have been studied by Tsuda et al.[13] They attached a strain gauge to a carbon fibre specimen, which was then connected to a digital oscilloscope that recorded the strain signal. Their results showed that the interference signal recorded during loading has a wide frequency range where vibrations are induced by contact of the specimen with hammer and testing fixture. In addition, Ouk and Seong[14] studied the dynamic fracture characteristic of a tungsten carbide cobalt composite material, and found that lower impact velocity value can increase the impact duration time of the specimen.

In order to correlate the impact energy, the current study focuses on the aluminium 6061-T6 material, which is widely used in many engineering structural applications. It boasts of superior mechanical properties, i.e., high strength of weight ratio, ideal ductility, excellent weld ability, high resistance to corrosion, corrosion cracking and deformability. The aluminium alloy 6061-T6 is a heat treatable, wrought Al–Mg–Si alloy. Magnesium and silicon are added either in balanced amounts to form quasi-binary Al–Mg_2Si, or with an excess of silicon needed to form Mg_2Si precipitate[15,16]. Injuries in crashes involving sport utility vans can be reduced as much as 26% using aluminium or lightweight material in vehicle design, along with slightly longer energy absorbing crush zones[17]. Aluminium can absorb twice the amount of energy compared with steel. Vehicles using aluminium can be safer by making them large enough to extend crush space for crash protection; at the same time, reducing weight can also boost fuel economy. Moreover, aluminium can be designed to fold predictably during a crash by allowing the vehicle to absorb most of the crash energy[17,18]. For example, aluminium alloy 6061-T6 has been used as the vehicle rim; thus, it directly experiences the impact load when the vehicle is moving on the road. However, one of the problems that arise in using this alloy is reduced durability leading to component failure. Compared with those made of steel, alloy rims made from aluminium 6061-T6 are easily damaged, fractured, and destroyed. This disadvantage may create a significant problem for drivers who find out later that they have to change their vehicle rims wheel to spend the money for potential costly repairs[18].

Wheel design and development division operates three major test wheel tests of rotary bending test, the radial fatigue test, and impact tests to the prototype for the consideration of the impact of various fatigue and durability considerations. The impact test is designed to evaluate the impact damage on the wheel when it hits a curb[18,19]. Velocities recorded when a wheel hits a curb may vary depending on the speed of a vehicle and the thickness of the wheel's wall. Two different velocities at 5.18 (18.65 km/h) and 3.35 m/s (12.06 km/h) seem to be similar to the instrument Charpy impact machine[20]. Thus, we were inspired by the idea of proceeding with further research using the signal processing approach.

From the literature, such as the study of Francois and Pineau[5], we know that the total absorbed energies using dial indicator and optical encoder differ by a significant amount. Hence, from related sources[12,14,21], different velocities and thicknesses were studied in the present research in order to indentify the durability of aluminium 6061-T6 wheel using a different parameter. Few studies have focused on

failure mode by means of Charpy impact loading using strain signal. The correlation between energy absorbed and strain energy from power spectrum density (PSD) must be studied to determine whether the dial/encoder absorbed energy can be replaced with energy using the signal processing approach.

From the overview and the problem statement previously highlighted, the main objective of the current study is to investigate the correlation between absorbed energy and strain energy from PSD as well as determine the strain response pattern with different velocities and thicknesses for aluminium 6061-T6. To achieve this goal, PSD analysis was performed using vibration energy distribution in order to clarify the behaviour. The input data of the PSD method consisted of impact signals obtained from the experimental work. The expected result (i.e., the correlation between vibration energy from PSD and absorbed energy) can be correlated with polynomial equation, in which the energy from PSD is related to the absorbed energy.

Theoretical Background

Charpy impact energy

Impact energy defines as the energy necessary to fracture a standard test piece under an impact load. The most common measurement of impact energy is the Charpy impact test. The energy absorbed in breaking the specimen is determined from a dial indication of the change in the height of the pendulum before the impact and after the specimen is broken. Alloys with large yield strength, maximum strength, and ductility (percent elongation at fracture) values have large impact fracture energies. Other methods of validating Charpy fracture energy have been performed, utilizing changes in kinetic energy from measurement of velocity both before and after fracture[22]. The impact velocity when the pendulum strikes at the specimen refer location (2) (as shown in Fig. 1) is given by Eq. (1):

$$v = \sqrt{2gH_1}, \quad \ldots (1)$$

where g is the acceleration due to gravity, and H is the change in elevation of the center of strike. The energy absorbed by the specimen while it is breaking (i.e., the impact energy) is an energy loss to the pendulum given by Eq. (2). Hence, this loss can be measured from the difference in the potential energy of the pendulum between the zero velocity points at locations (1) and (3), as shown in Fig. 1:

$$U = mg\,(h_1 - h_3) = mgr\,(\cos\beta - \cos\alpha), \quad \ldots (2)$$

where m is the pendulum mass, and h_1 and h_3 are the elevations of the center of mass; moreover, the center of mass is located at a distance r from the center of rotation[23].

Power spectral density

PSD matrix function approximation of the response of non-linear multi-degree of freedom mechanical system with damping can be obtained using the equivalent linear system method[8]. A PSD is a normalized density plot shows the mean square amplitude of each sinusoidal wave with refer to its frequency. It presents the vibration energy distribution of the signal across the frequency domain. PSD function shows the strength of the variations (energy) as a function of frequency. The energy can be obtained within a specific frequency range by integrating PSD within that frequency range. Francois and Pineau[5] calculated the vibration energy from the accelerometer data using Fourier analysis and compared the energy with a dial indicator and optical encoder.

PSD matrix function of the nonlinear response is defined as the PSD of the stationary response of the equivalent linear system which this approach involves complicated numerical analysis[8]. The autocorrelation function and power spectrum have similar measurements in the domain time and frequency. Both functions can be related to the Fourier transform function using the fast Fourier transform (FFT). The PSD can then be calculated using the following formula[24,25,31]:

$$P_{xx}(\omega) = \frac{1}{2\pi}\int_{-\infty}^{\infty} r_{xx}(\tau)e^{-j\omega t}\,d\tau \quad \ldots (3)$$

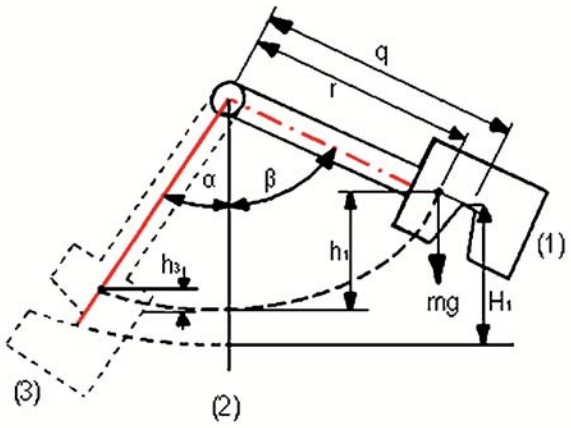

Fig. 1—The sketch of charpy impact absorbed energy theory

The relationship between the autocorrelation functions is given as:

$$r_{xx}(\tau) = \int_{-\infty}^{\infty} x(t)\, x(t-\tau)\, dt \quad \ldots (4)$$

The power spectrum function is usually an even function of ω and the autocorrelation function is usually an even function for τ. This integration can be stated as:

$$P_{xx}(\omega) = \frac{1}{2\pi} \int_{-\infty}^{\infty} r_{xx}(\tau) kos(\omega\tau)\, d\tau \quad \ldots (5)$$

where

$$r_{xx}(\tau) = 1/2\pi \int P_{xx}(\omega)\, kos(\omega\tau)\, d\omega = 1/\pi \int P_{xx}(\omega)\, kos(\omega\tau)\, d\omega \quad \ldots (6)$$

The power spectrum function, $P_{xx}(\omega)$, provides information related to the average power for the signal component; meanwhile, the frequency spectrum, $G(j\omega)$, is defined as the amplitude and the phase angle. The relationship between $P_{xx}(\omega)$ and $G(j\omega)$ can then be stated as:

$$P_{xx} = |G(j\omega)|^2 \quad \ldots (7)$$

Natural frequencies of the striker arm system

Natural frequency is the frequency with which the striker arm system oscillates without external forces. After an initial disturbance, the system is left to vibrate on its own[25]. From the study of Shterenlikth *et al.*[8] the first natural frequency of the striker arm system, which is calculated using the Eq. (8), can be shown with the main peak of PSD. As previously discussed, energy can be measured from the area under PSD curve. By using Timoshenko beam theory the natural frequencies of the striker arm system can be measured[8]. The striker arm is presented as a simply supported beam of constant cross-section. Figure 2 shows the striker attached to one end of the beam. The beam deflections are shown in the following form:

$$y = X(x)(A \cos pt + B \sin pt), \quad \ldots (8)$$

where p is equal to the angular frequency of vibration.

After a few steps, the following frequency equation is obtained:

$$\frac{\rho A l^2}{J} = \frac{(kl)^3}{2} \left(\frac{1}{\tanh kl} - \frac{1}{\tan kl}\right), \quad \ldots (9)$$

where A is cross-section of the striker arm, ρ is material density of striker arm, l is length of striker, and J is mass moment of inertia. In this case, the ρ and l values were set at the point of 7.87×10^3 kg/m^3 and 0.8 m, respectively. Therefore, the first three roots of Eq. (10) calculated for $k_1 l = 2.098$, $k_2 l = 4.052$, and $k_3 l = 7.090$. The natural frequencies can be calculated using the following equation:

$$\omega^2 = k^4 \frac{EI}{\rho A}, \quad \ldots (10)$$

where $I = \frac{bh^3}{12}$ (b = width and h = height of specimen).

Finally, natural frequencies of the striker arm system[8] is equal to $f_i = \omega/2\pi$, $f_1 = 84$ Hz, $f_2 = 314$ Hz, and $f_3 = 960$ Hz.

Impact duration

Impact is the collision between two bodies, which occurs within a very short period of impact duration in a very small interval of time. In perfectly elastic collision, the interaction between the colliding solids can be shown by a contact spring where stiffness of spring increases the impact force, thereby reducing the impact duration[26]. In the real situation, the impact duration is important, and a vehicle made of material with higher impact duration is safer; this is also complemented by a larger area that extends crush space for crash protection.

From the problem of impact of two bodies

$$(\dot{\alpha}^2 - v^2) = -\frac{4}{5} Mn\alpha^{\frac{5}{2}}, \quad \ldots (11)$$

or solving for $\dot{\alpha}$ and generalizing the above equation[27] by replacing n with n^1, we have:

$$\dot{\alpha} = \left(v^2 - \frac{4}{5} Mn^1 \alpha^{\frac{5}{2}}\right)^{1/2} \quad \ldots (12)$$

Substituting $\dot{\alpha} = d\alpha/dt$ in Eq. (12) and solving for dt:

$$dt = \frac{d\alpha}{\left(v^2 - \frac{4}{5} Mn^1 \alpha^{\frac{5}{2}}\right)^{1/2}}. \quad \ldots (13)$$

Combining Eq. (13) with $\alpha_1 = \left(\frac{5v^2}{4Mn^1}\right)^{2/5}$ and then performing integration gives

$$t = \frac{2\alpha_1}{v} \int_0^x \frac{dx}{(1 - x^{\frac{5}{2}})^{1/2}}, \quad \ldots (14)$$

where $x = (\alpha/\alpha_1)$. The total impact duration, t_o, is obtained by integrating between the limits x=0 and x=1 and is given as:

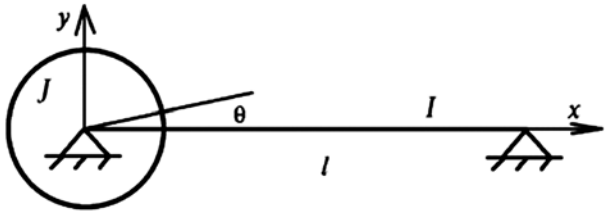

Fig. 2—Mechanical model of the striker arm system with simply supported beam[8]

$$t_o = 2.94\frac{\alpha_1}{v} = 2.94\left(\frac{5}{4Mn^1v^{1/2}}\right)^{2/5}, \quad \ldots (15)$$

where $M = \frac{1}{m_1} + \frac{1}{m_2}$ … (16)

(M = total mass, m_1 = mass impactor, m_2 = mass specimen, v = velocity during impact), and

$$n^1 = \frac{4\sqrt{R_1}}{3\pi(k_1+k_2)} \quad \ldots (17)$$

where $k_1 = \frac{1-v_1^2}{\pi E_1}$ ... (18)

and $k_2 = \frac{1-v_2^2}{\pi E_2}$ ... (19)

where v_1 = striker poisson ratio, v_2 = specimen poisson ratio, R_1 = radius of a spherical striker,

E_1 = striker Young Modulus dan E_2 = specimen Modulus Yong.

Methodology

The material used throughout this research is aluminium 6061-T6, which is run in room temperature and free from the temperature effect. The properties of the specimen and the striker are presented in Table 1. The density and the Poisson's ratio values shown in Table 1 were taken from related literature. In addition, the values of yield stress, ultimate stress, and Young's Modulus were obtained from the actual laboratory tensile test performed earlier by the authors[28].

Two strain loadings were captured using the 2 mm strain gauge with 120 ohm resistance. For this purpose, the strain gauges were attached to the striker during and connected to the specific data acquisition system during the testing. The applied sampling rate throughout the experiment was maintained at 50 kHz. This is an appropriate data range, in which the normalised PSD of acceleration signals always occurs within the range[8]. Moreover, because impact occurs between a millisecond, with a sample rate of 50,000 Hz, there should be 50 data collections for one millisecond. The obtained values were then plotted on a graph. The Charpy impact apparatus with the location of strain gauges at the striker and data acquisition is shown in Fig. 3. The standard Charpy impact specimen with the dimensions of 10 mm × 10 mm × 55 mm in depth, width and length, respectively, was designed according to ASTM E23[23]. The geometrical drawing of the specimen is shown in Fig. 4. In this study, two types of thicknesses were used with the dimensions 10 mm and 5 mm, respectively.

Both Charpy apparatus and data acquisition were calibrated in order to ensure the accuracy of the results or impact responses collected. The dial energy of the Charpy machine was adjusted at the zeroing value for the purpose of initiating the experiment. In the present research, two types of velocities were used (i.e., 5.18 m/s and 3.35 m/s) similar with the Charpy impact machine specification with the high latch and low latch velocities of 5.18 and 3.35 m/s, respectively. These different velocities were used as guidelines via signal processing approach. The

Table 1—Properties of material for striker and Charpy specimen

Component	Material	Yield stress σ_y (MPa)	Ultimate stress σ_u (MPa)	Young's modulus, E (GPa)	Density, ρ (kg/m^3)	Poisson's ratio, υ
Striker	Steel	-	-	200	7.86×10^3	0.32
specimen	Alum 6061-T6	292	328	70	2.71×10^3	0.35

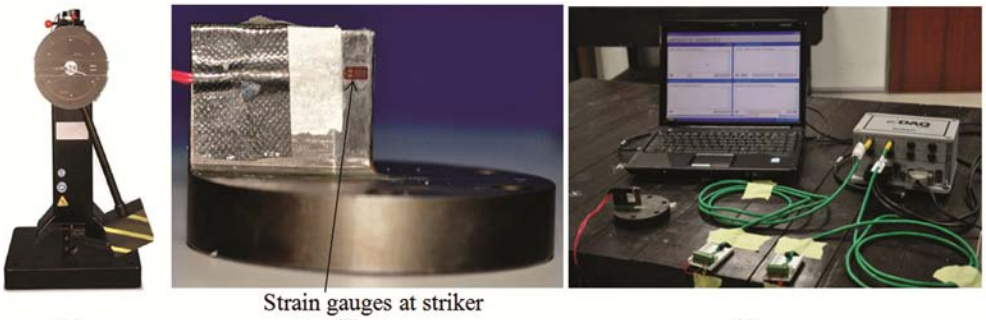

Fig. 3—Equipment used for the Charpy impact test: (a) instrument Charpy impact, (b) Charpy impactstriker and (c) data acquisition equipment

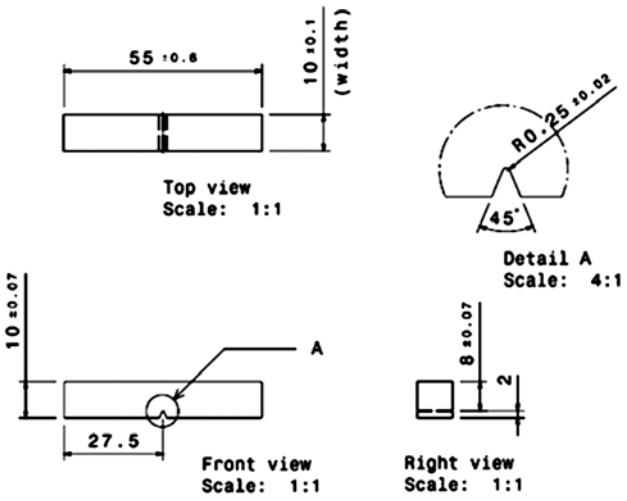

Fig. 4—Detail drawing for Charpy impact specimen

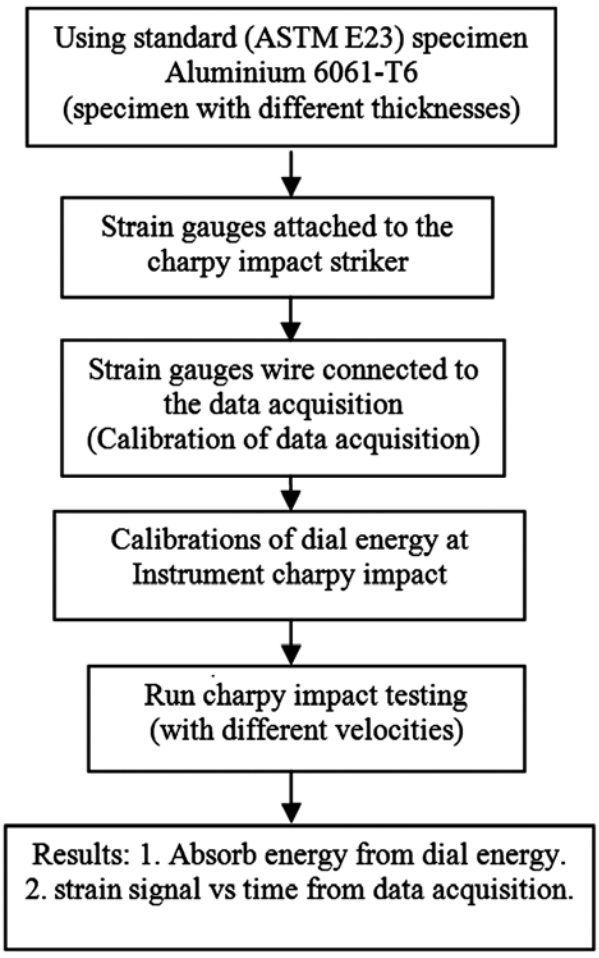

Fig. 5—The flow of the implemented Charpy impact testing

process flow of the Charpy impact testing procedure is presented in Fig. 5. After collecting the response signals obtained in the impact, for which the signal was presented in the form of time series, those signals were then analysed to clarify the behaviour of the data sets using PSD. As such, the distribution trend of the vibration energy in the frequency domain were properly observed and analysed. Finally, the correlation between energy absorbed from dial indicator and the calculated energy obtained from the PSD analysis were performed, leading to the core element of this research.

Results and Discussion

Figures 6-9 show the plotted time history of strain signal based on sinusoidal shape[29] and PSD plots for different values of velocity and thickness. As can be seen, both velocities at the highest amplitude of PSD for 10 mm are higher than 5 mm. Generally, this indicates that the velocity and thickness can give the effect to the PSD. From Figs 6 and 7, it can be seen that for 10 mm thickness (velocity 5.18 m/s) the strain versus the time gave higher maximum strain value compared with the 5 mm thickness. The average PSD peak value obtained from all five experiments was approximately 147.4 $\mu\varepsilon^2$/Hz for the 10 mm thickness

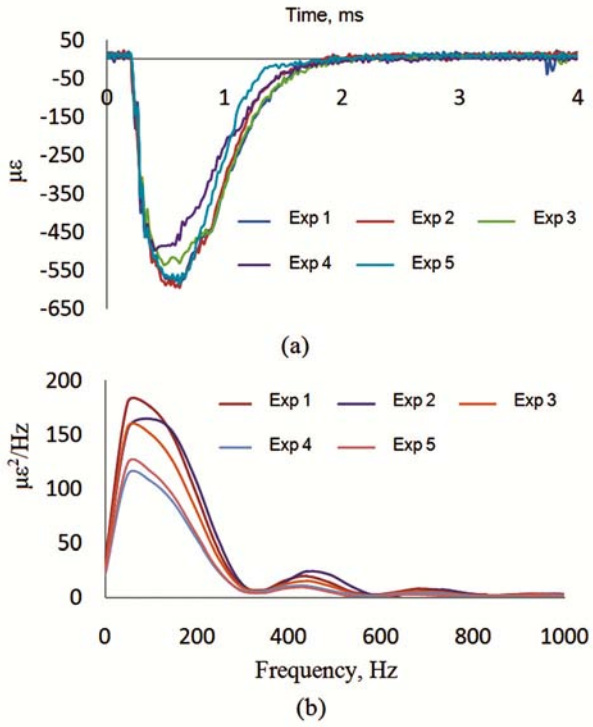

Fig. 6—The distribution for velocity 5.18 m/s and 10 mm thickness: (a) time histories and (b) PSD

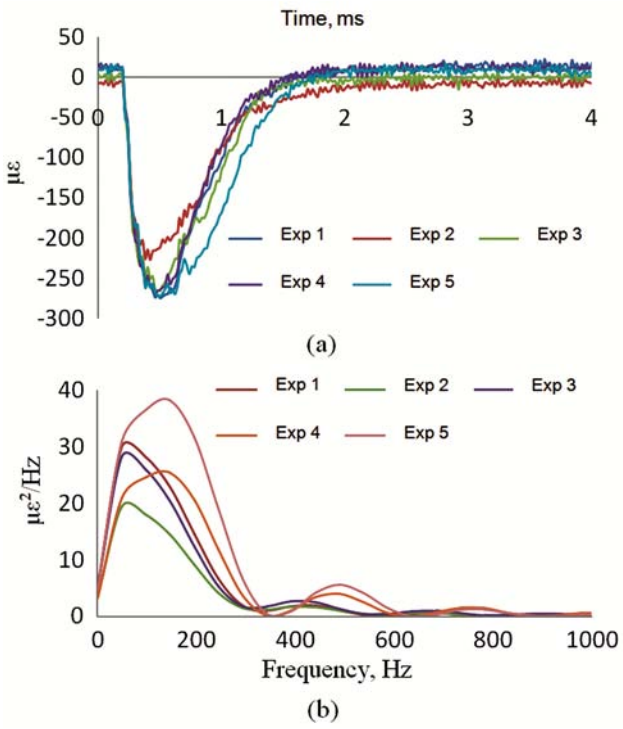

Fig. 7—The distribution for velocity 5.18 m/s and 5 mm thickness: (a) time histories and (b) PSD

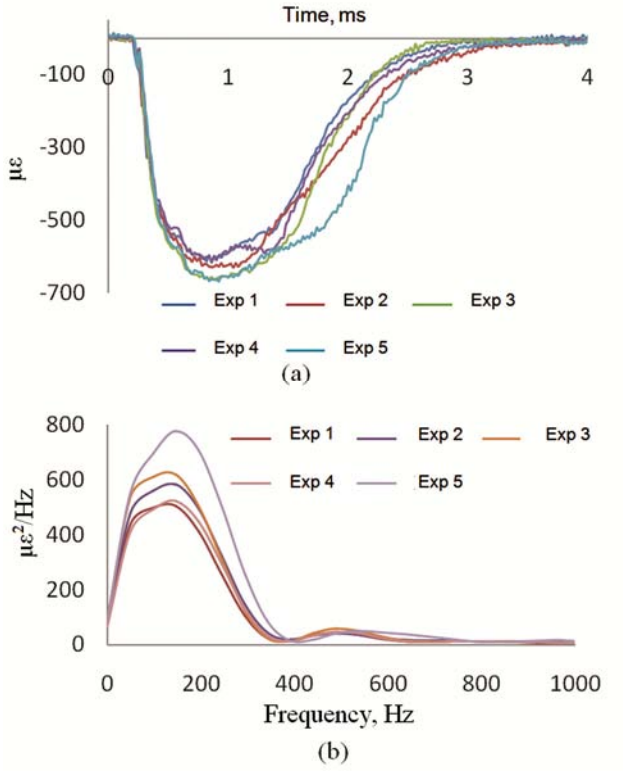

Fig. 8—The distribution for velocity 3.35 m/s and 10 mm thickness: (a) time histories and (b) PSD

and 28.3 με²/Hz for the 5 mm thickness at the first dominant (Table 2). From the results of time histories and PSD, the 10 mm thickness provided higher maximum strain and PSD peak values compared with the 5 mm thickness. In addition the energy under the area of the PSD graph (velocity 5.18 m/s) for 10 mm thickness was larger than that for the 5 mm thickness. There exists a relationship between load calibration factor and specimen thickness; moreover, the instrument striker must be calibrated for different thicknesses and materials to ensure accurate impact load data[21].

For Figs 8 and 9, the trend was the same (i.e., higher thickness gave higher strain value). This is because higher specimen thickness need more energy to fracture the specimen, thereby affecting the vibration of impact striker and increased the value of maximum strain. Based on the study by Nazari and Didehvar[30] the impact resistance (energy) of the specimens depends on the number of layers (specimen thickness). As can be seen, for the 10 mm thickness (velocity 3.35 m/s) the strain versus the time gave higher maximum strain value compared with the 5 mm thickness. The average PSD peak value obtained from all five experiments was approximately 600.9 με²/Hz for the 10 mm thickness and 84.9 με²/Hz

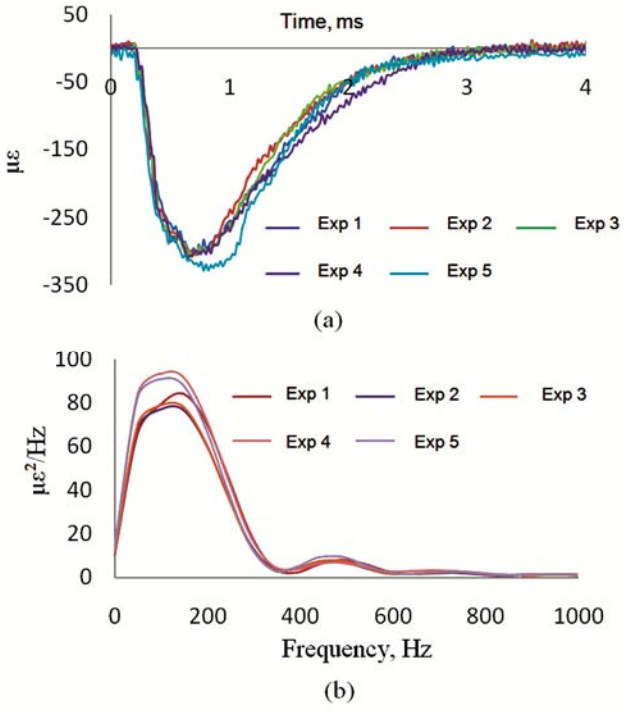

Fig. 9—The distribution for velocity 3.35 m/s and 5 mm thickness: (a) time histories and (b) PSD

Table 2—The PSD peak ($\mu\varepsilon^2$/Hz) and different percentage with different velocities and thicknesses

Exp. no.	Velocity 5.18 m/s		Velocity 3.35 m/s	
	10 mm thickness (G1)	5 mm thickness (G2)	10 mm thickness (G3)	5 mm thickness (G4)
1	179.6	30.07	503.9	84.34
2	164.4	19.49	583.2	77.08
3	156.8	28.31	618.1	78.82
4	112.9	25.38	522.6	93.41
5	123.5	38.21	776.9	90.95
Average	147.4	28.3	600.9	84.9
% Difference	421%	0%	2023%	200%

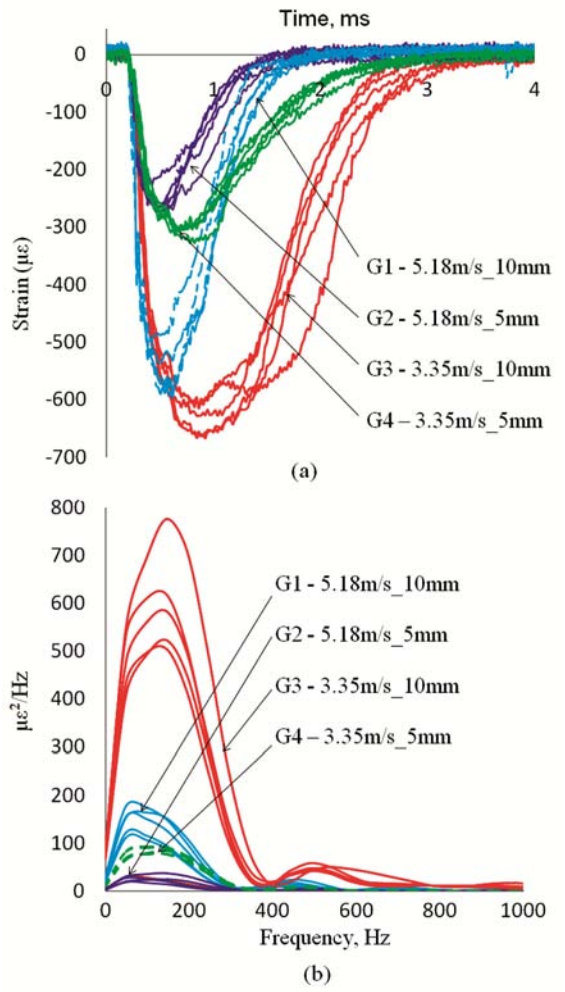

Fig. 10—The distribution for all velocities and thickness: (a) time histories and (b) PSD

for the 5 mm thickness at the first dominant (Table 2). From the results of time histories and PSD, the 10 mm thickness provided higher maximum strain and PSD peak values compared with the 5 mm thickness.

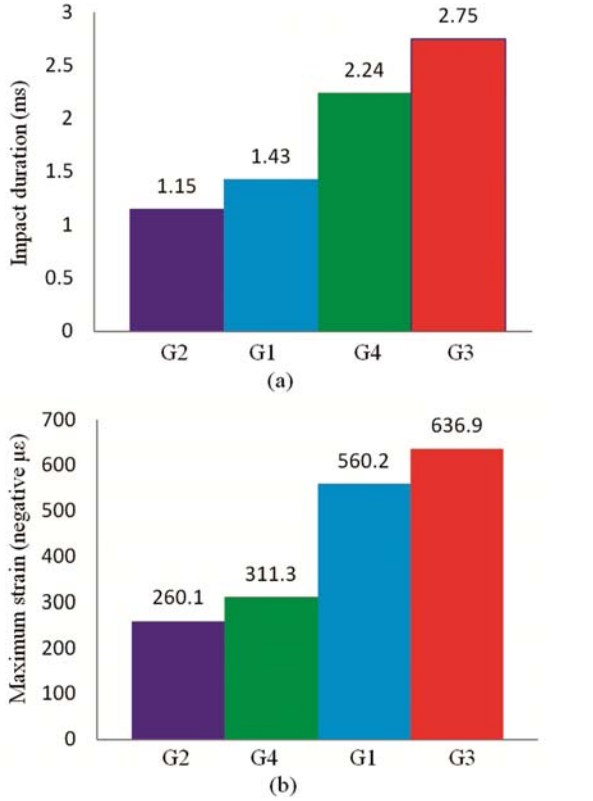

Fig. 11—The distribution for (a) impact duration and (b) maximum strain

From the results of Figs 6-9 for both velocities (5.18 and 3.35 m/s) the PSD peak for 10 mm thickness higher than that for the 5 mm thickness (Table 2). This is because from the theory referring to Eq. (10)[8], natural frequency depends on the moment of inertia; in turn, the moment of inertia depends on the thickness of the material. The natural frequency increases as the thickness increases, wherein the PSD is proportional to natural frequency. Shterenlikth *et al.*[8] showed that the natural frequency can be demonstrated using the PSD peak.

Table 3—Impact duration and maximum strain with different velocities and thickness

Exp. no.	Velocity 5.18 m/s				Velocity 3.35 m/s			
	10 mm thickness (G1)		5 mm thickness (G2)		10 mm thickness(G3)		5 mm thickness(G4)	
	Duration, ms	Max strain, με	Duration, ms	Max strain, με	Duration, ms	Max strain, με	Duration, ms	Max strain, με
1	1.46	-588.7	1.18	-274.0	2.64	-614.9	2.18	-304.7
2	1.46	-594.5	1.10	-264.6	3.02	-627.9	2.32	-304.7
3	1.56	-535.4	1.12	-268.2	2.36	-662.8	2.2	-307.9
4	1.44	-496.7	1.02	-221.8	2.86	-612.0	2.34	-311.8
5	1.24	-585.8	1.32	-271.7	2.88	-666.9	2.16	-327.5
Average	1.43	-560.2	1.15 ms	-260.1	2.75	-636.9	2.24	-311.3
% Diff.	24%	115%	0%	0%	139%	145%	109%	20%

Table 4—Absorbed energy and strain energy with different velocities and thickness

Exp. no.	Velocity 5.18 m/s				Velocity 3.35 m/s			
	10 mm thickness (G1)		5 mm thickness (G2)		10 mm thickness (G3)		5 mm thickness (G4)	
	Absorbed energy, J	Strain energy, $\mu\varepsilon^2$	Absorbed energy, J	Strain energy, $\mu\varepsilon^2$	Absorbed energy, J	Strain energy, $\mu\varepsilon^2$	Absorbed energy, J	Strain energy, $\mu\varepsilon^2$
1	20	34027	10	5418	30	112610	18	18596
2	20	33258	10	3479	36	131990	17	17146
3	20	29254	10	4944	38	137850	17	17342
4	20	20657	10	5406	36	116550	19	20688
5	20	22106	10	8232	42	177490	17	19515
Average	20	27860	10	5496	36.4	135298	17.6	18657
% Diff	100%	407%	0%	0%	264%	2362%	76%	239%

The findings of the strain distribution of all experiments and the corresponding PSD plots are shown in Fig. 10. Strain versus time velocity of 3.35 m/s with 10 mm thickness (G3) gave the highest maximum strain value, followed by G1, G4, and G2. Table 4 shows that compared with G2, the value of the different percentage of G3 is 145%; this is followed by 115% and 20% for G1 and G4, respectively. Figure 11 shows the plot for the impact duration and maximum strain for different velocities and thicknesses. The highest value for impact duration and maximum strain are found at $v = 3.35$ m/s with $t = 10$ mm, with 2.75 ms and 636.9 microstrain, respectively.

G3 gave the highest impact duration value, followed by G4, G1, and G2. This shows that the highest impact duration occurs at the lower velocity with higher thickness (3.35 m/s with the 10 mm thickness). This is because aluminium has ideal ductility, will increase the impact duration at lower velocity. Another reason is higher specimen thickness needs more energy to fracture the specimen and it will influence the impact duration. Table 3 also shows that the value of different percentage of G3 is 139%, followed by 109% and 24% for G4 and G1, respectively, compared with G2. With lower velocity, aluminium can absorb slightly longer energy crush zones. Based on Eq. (15), the impact duration increases as the velocity decreases, in which the impact duration is inversely proportional to velocity. From related research[14], the decrease of impact velocity leads to increased fracture time. The impact duration is also inversely proportional to total mass as shown in Eq. (16); at the same time, it is proportional to mass[27], where the mass is dependent on the thickness of material.

As for PSD, the highest value was obtained by G3, followed by G1, G4, and G2. Table 2 shows that the value of different percentage of G3 is 2023%, followed by 421% and 200% for G1 and G4, respectively, compared with G2, indicating that G3 has the highest value of strain and impact duration. G2 has the lowest PSD value because G2 has the lowest maximum strain and impact duration. This shows that the PSD value is dependent on strain value and impact duration value. Moreover, when the strain

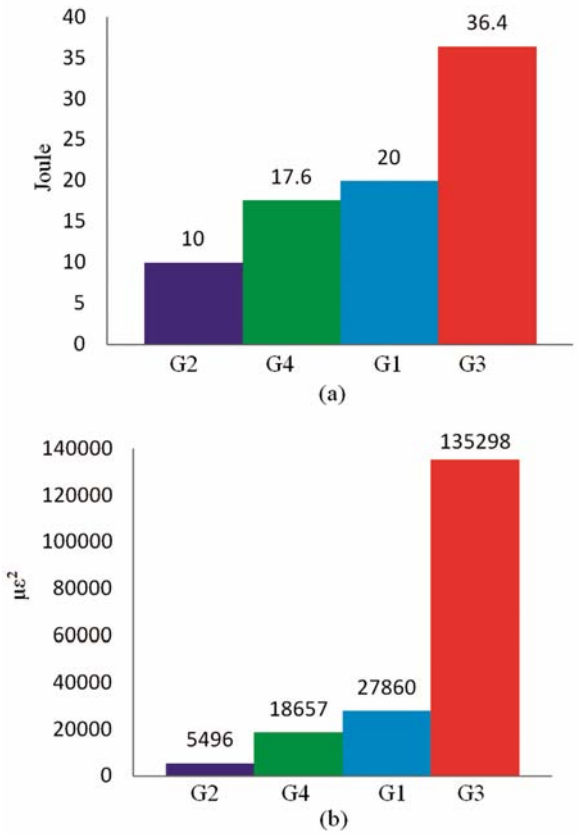

Fig. 12—The distribution for (a) absorbed energy and (b) strain energy

value and impact duration are higher, the area below the graph for strain versus time becomes higher, thus affecting PSD value. Nuawi *et al.*[31] have reported that higher amplitude and signal frequency can lead to higher PSD value.

Table 4 shows the experimental result for the absorbed energy and strain energy with different velocities and thicknesses. As can be seen, the highest value for both energies occurred at a velocity of 3.35 m/s with 10 mm thickness (G3), followed by 5.18 m/s with 10 mm thickness (G1), 3.35 m/s with 5 mm thickness (G4), and 5.18 m/s with 5 mm thickness (G2). Figure 12 shows the distribution for absorbed energy and strain energy in relation to velocities with different thicknesses. From the graph, it can be seen that the patterns of both energies are similar, where the lowest and highest energies occurred at 5.18 m/s with 5 mm thickness and 3.35 m/s with 10 mm thickness, respectively. The pattern of the graphs and the values of the different percentages show a relationship, in which the value of absorbed

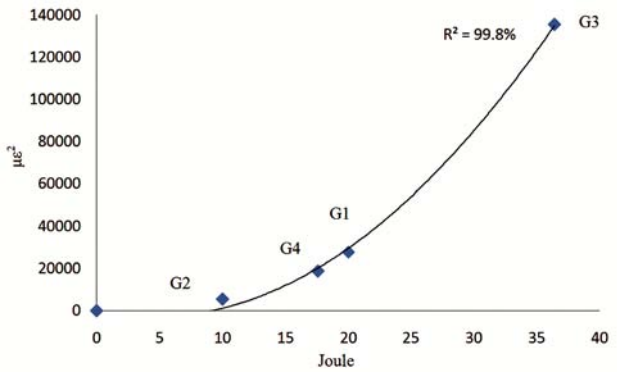

Fig. 13—The curve for energy from PSD versus energy absorbed

energy is proportional to the strain energy. This can be explained by the fact that a higher value of absorbed energy can affect the vibration of the striker. In turn, when the vibration of striker is higher, the value of strain signal also becomes higher, thus affecting the value of strain energy. A previous study has reported that absorbed energy depends on yield strength and maximum strength; moreover, ductility and absorbed energy can be calculated under the total area of the load-displacement curve[22]. In additional failure patterns depend strongly on the impact energy[29].

The correlation between strain energy and energy absorbed for all experiments is shown in Fig. 13. As can be seen, higher energy absorbed leads to higher strain energy; moreover, the energy absorbed is related to the strain energy. With a correlation coefficient (R^2) of 98.8%, we can assume that there exists a strong relationship between these two energies. R^2 is the square of the correlation between the response values and the predicted response values; this is between 0 and 1, and a value closer to 1 indicates that a greater proportion of variance is accounted for by the model. The relationship energy absorbed strain energy with polynomial correlation. The polynomial correlation has been chosen because the impact energy is affected by or related to vibration energy. From the study by Francois and Pineau the energy of an instrumented striker by calculating the vibration energy (accelerometer data) using Fourier analysis is influenced or related to the absorbed energy[5]. The study with Xu *et al.*[7] which is in accordance to ASTM, more than 80% of the absorbed energy is not accurate and calculated as an estimate.

Conclusions

This paper discussed the correlation of impact energy with absorbed energy and strain energy using

instrumented Charpy impact. From the experimental result, it can be concluded that the PSD value is dependent on strain value and impact duration value; particularly, the PSD value is higher when the strain value and impact duration are higher. The velocity and thickness can affect the absorbed energy, and this parameter is important in testing the material. Based on our experiment, with higher velocity and lower thickness, this material is easily damaged and fractured compared with lower velocity and higher thickness.

The correlation energy from PSD and energy absorbed shows that the higher energy absorbed leads to a higher strain energy, as shown in polynomial relationship with R square of 99.8%. This means that the energy absorbed is related to the strain energy calculated from the area under PSD. This correlation can replace the dial/encoder absorbed energy with energy using signal processing approach. This finding also verifies the suitability of strain energy from PSD and suggests that related experiments can be used apart from the Charpy impact test to verify the impact energy accurately.

Acknowledgements

The authors would like to express their gratitude to Universiti Kebangsaan Malaysia grant UKM-KK-03-FRGS 0118-2010 and Universiti Teknikal Malaysia Melaka for supporting these research activities.

References

1 Francois D & Pineau A, *Studies toward Optimum Instrumented Striker Design, From Charpy to Present Impact Testing* (Elsevier Science Ltd. and ESIS) 2002, 9.

2 Rossoll A, Berdin C & Prioul C, *Int J Fract*, 115 (2002) 205-226.

3 Kondryakov E A, Zhmaka V N, Kharchenko V V, Babutskii A I & Romanov S V, *Strength Mater*, 37 (2005) 3.

4 Jang Y C, Hong J K, Park J H, Kim D W & Lee Y, *J Mater Process Technol*, 201 (2008) 419-424.

5 Francois D & Pineau A, *Observations on Differences between the energy determined using an instrumented striker and Dial/Encorder Energy, From Charpy to Present Impact Testing* (Elsevier Science Ltd. and ESIS) 2002, 9.

6 Siewert T A & Manahan Sr M P, *The different between total absorbed energy measured using an optical encoder. Pendulum Impact Testing: A century of progress* (American Society for Testing and Materials, West Conshohocken, PA), 2000.

7 Xu S, Bouchard R & Tyson W R, *J Test Eva*l, 34(3)(2006) 176-180.

8 Shterenlikht A, Hashemi S H, Yates J R, Howard I C & Andrews R M, *Int J Fract*, 132 (2005) 81-97.

9 Toshiro K, Masahiro O, Shigeki M & Hiroyuki T, *J Iron Steel Inst Japan,* 86 (2000) 595-601.

10 Sahraoui S & Laitailate J L, *Eng Fract Mech*, 60(4) (1998) 437-446.

11 Kondryakov E A, Zhmaka V N, Kharchenko V V, Babutskii A I & Romanov S V, *Strength Mater*, 37 (2005) 3.

12 Aggag G & Takahashi K, *Polym Eng Sci*, 36 (1996) 17.

13 Tsuda H, Takeda S, Takahashi J & Urabe K, *J Mater Sci Lett*, 19 (2000) 1-2.

14 Ouk S L & Seong K H, *KSME Int J*, 11(5) (1997) 513-520.

15 Jogi B F, Brahmankar Technal,P K, Nanda V S & Prasad R C, *J Mater Process*, 201 (2008) 380-384.

16 16Toh C K & Kanno S, *J Mater Sci*, 39 (2004) 3497-3500.

17 *Automotive in aluminium*. www. autoaluminium.org

18 *Research activity case study, Structure Analysis for Alloy Rim utilizing Computer-Aided Engineering*, (Dream Edge Sdn. Bhd.), 2009.

19 Chang C L & Yang S H, *Eng Failure Anal*, 16 (2009) 1711-1719.

20 Impact Pendulum Test System Brochure S1-1 Specification. *www.instron.com.*

21 Francois D & Pineau A, *Problem related to the measurement of load signal in the instrumented charpy impact, From Charpy to Present Impact Testing* (Elsevier Science Ltd. and ESIS) 2002, 9.

22 Francois D & Pineau A, *Insrumented Charpy Test Review and Application to the Structure Integrity, From Charpy to Present Impact Testing* (Elsevier Science Ltd. and ESIS), 2002, 9.

23 *Charpy Pendulum Impact Test, International Standard Metallic Materials part 1, 2 and 3* (Department of Standards Malaysia) 2006.

24 Shiavi R, *Introduction to applied statistical signal analysis* (Academic press, San Diego), 1999, 2.

25 Singiresu S R, *Mechanical Vibrations* (Prentice Hall, Singapore), 2005.

26 Rajalingham C & Rakheja S, *J Sound Vibr*, 229(4) (2000) 823-835.

27 Zukas J A, Nicholas T, Swift H F, Greszczuk L B & Curran D R, *Impact Dynamics* (John Wiley & Sons, United Stated of America), 1982.

28 Kutz M, *Handbook of Materials Selection* (John Wiley & Sons, New York), 2002.

29 Daniel I M, Abot J L, Schubel P M & Lou J J, *Exp Mech*, (2011) doi: 10.1007/s11340-011-9479-y.

30 Nazari A & Didehvar N, *Composite: Pt B*, 42, (2011) 1912-1919.

31 Nuawi M Z, Noor M J M, Jamaluddin N, Abdullah S, Lamin F & Nizwan C K, *J Appl Sci*, 8(8) (2008) 1541-1547.